Thermochimica Acta 546 (2012) 102–112

Contents lists available at SciVerse ScienceDirect

Thermochimica Acta

journal homepage: www.elsevier.com/locate/tca

The application of the formalism of dispersive kinetics for investigation of the isothermal decomposition of zinc leach residue in an inert atmosphere

Bojan Janković[a,*], Srećko Stopić[b], Aybars Güven[b], Bernd Friedrich[b]

[a] Faculty of Physical Chemistry, University of Belgrade, Studentski trg 12-16, P. O. Box 137, 11001 Belgrade, Serbia
[b] IME Process Metallurgy and Metal Recycling, RWTH Aachen University, Aachen, Germany

ARTICLE INFO

Article history:
Received 23 April 2012
Received in revised form 10 July 2012
Accepted 11 July 2012
Available online 20 July 2012

Keywords:
Zinc leach residue
Dispersive kinetics
Distribution of the apparent activation energy
Secondary nucleation process

ABSTRACT

Formalism of dispersive kinetics is applied for the decomposition process of zinc leach residue in an inert atmosphere. Thermal decomposition has been studied in a tubular furnace under a constant nitrogen gas flowing, at four different operating temperatures. It was found that the presented dispersive kinetic model can much better describe the complex decomposition process than classic Šesták-Berggren kinetic model. It was shown, that increase in the values of dispersive parameter (θ) leads to an increase in dispersion of conversion values, together with the appearance of the distribution of the apparent activation energies. It was established that several parallel elementary reactions with strictly defined, but different apparent activation energies, contribute to the overall decomposition process. The model presented in this article may offer a more physically meaningful approach for the treatment of the kinetic data for the investigated process, compared to that of standard (i.e., non-dispersive) kinetic model.

1. Introduction

The classical chemical kinetics was formulated for isolated reactions in homogeneous, three-dimensional systems [1]. However, this approach fails in the solids [2,3]. The basic classical kinetic equation to describe the processes in the solid state can be represented in the form:

$$\frac{d\alpha}{dt} = kf(\alpha) \quad (1)$$

where α is the degree of conversion or the extent of reaction, t is the reaction time, k is the specific reaction rate (the rate constant), while $f(\alpha)$ represents the proper function for a given reaction model [4], which describes the decomposition process. In practical cases, the analytical form of the function $f(\alpha)$ usually corresponds to the first order reaction kinetics.

$$f(\alpha) = (1 - \alpha). \quad (2)$$

Formally, the use of Eq. (1) is equivalent to a change of reaction order. In common practice, in that way one recovers the constant specific reaction rate or the rate constant of classical kinetics and tries to describe its temperature-dependence by the Arrhenius equation. From the variety of kinetic model functions $f(\alpha)$, one can usually choose the proper one [5], to fit a given set of experimental data, but sometimes one finds it necessary to use more than one function for the same system differing only in crystallite sizes or the amount of structural defects. The numerical values of the rate constants are the model-dependent.

In addition, the deviations from the Arrhenius equation are quite common, most probably due to the difference between the idealized process assumed in formulating the kinetic model function and the actual process in the investigated system. To account for these deviations the kinetic model function may be multiplied by some empirical function accommodating the distortion of the actual process from the idealized model [6,7].

Dispersive kinetics [3] sometimes referred to as distributed kinetics or stochastic kinetics, is underpinned by the concept of a distribution of the apparent activation energies. The apparent activation energy distribution (as opposed to the single *activation energy* that is typically inferred via inspection of the Arrhenius/Eyring equation) is simply a manifestation of system heterogeneity that can cause, for example, a reactant species to become less reactive as a given conversion proceeds [8]. Such a change in the apparent reactivity can come about as a result of local structural relaxation that occurs in parallel with the overall conversion; these continuous environmental renewals (i.e., system dynamics) can impact the kinetics if they occur on a time scale that is similar to, or slower than, the conversion under investigation. Note, however, that in the event that the system renewals occur significantly faster than the conversion, the dispersive kinetics paradigm simply reverts back to the classical kinetics one, whereby the activation energy distribution collapses into a Dirac delta function (as such,

* Corresponding author. Tel.: +381 11 2187 133; fax: +381 11 2187 133.
E-mail address: bojanjan@ffh.bg.ac.rs (B. Janković).

0040-6031/$ – see front matter © 2012 Elsevier B.V. All rights reserved.
http://dx.doi.org/10.1016/j.tca.2012.07.012

the development of rational dispersive kinetic treatments should account for that behavior).

Dynamical processes in which many timescales coexist are called *dispersive*. The rate constants for dispersive processes depend on time. In the case of a chemical reaction, the time dependence of the rate constant, $k(t)$, termed the specific reaction rate, is rationalized in the following way: Reactions by their very nature have to disturb reactivity distributions of the reactants in the condensed media, as the more reactive species are the first ones to disappear from the system. The extent of this disturbance depends on the ratio of the rates of reactions to the rate of internal rearrangements (mixing) in the system restoring the initial distribution in reactivity of reactants. If the rates of chemical reactions exceed the rates of internal rearrangements, then the initial distributions in reactant reactivity are not preserved during the course of reactions and the specific reaction rates *depend* on *time*.

Dispersive effects have been reported in the spectroscopy of single molecules [9,10] (even of those in highly ordered environments, such as on crystal surfaces studied under UHV conditions [11]) and, similarly, in the non-exponential (i.e., non-Maxwell-Debye relaxation) blinking kinetics of quantum dots [12]. Relaxation times in polymeric systems, crystal thermolyses, diffusion-limited reactions, protein folding, certain crystallizations, and vitrification can also exhibit dispersive kinetics [13]. Dispersive transport is often considered the underlying phenomenon responsible for the observation of dispersive kinetics in traditional (i.e., not ultra-fast) conversions. The Fokker-Planck (FP) equation can be used to relate the probability density function ((*pdf*)) for Brownian motion in the presence of an external force field caused by a given potential surface.

The intrinsic property of kinetics [3], as well as the transport and relaxation [14] in disordered systems is the time scale invariance: there is no one characteristic time scale the processes proceeds on all experimentally accessible time scales. This phenomenon is accounted for by the use of fractal time, t^{λ}, with $0 < \lambda < 1$. Fractal time is introduced into the kinetic equations by means of a time-dependent specific reaction rate of the form:

$$k(t) = \left(\frac{\lambda}{\zeta}\right)\left(\frac{t}{\zeta}\right)^{\lambda-1} \tag{3}$$

Using this form of time-dependent specific reaction rate, we can evaluate from Eq. (4)

$$-\frac{\mathrm{d}(1-\alpha)}{\mathrm{d}t} = k(t)(1-\alpha) \tag{4}$$

where $(1-\alpha)$ represents the fraction of starting material remaining in the system at time t) after the integration procedure, the equation in the following form:

$$\alpha = 1 - \exp\left[-\left(\frac{t}{\zeta}\right)^{\lambda}\right]. \tag{5}$$

It should be noted the universal form of Eq. (5). For $\lambda = 1$, Eq. (5) corresponds to the textbook form of the kinetic equation for the first-order reaction. For $1 < \lambda < 4$, Eq. (5) can be identified with Avrami equation [15,16] used to describe the sigmoid α versus t curves for the reaction in solids. In the field of physics, term $\exp[-(t/\zeta)^{\lambda}]$ for $0 < \lambda < 1$ is often referred to as the Kohlrausch relaxation function to describe the decay of a residual charge in Leyden jars. For $\lambda > 1$, Eq. (5) is also well-known as the Weibull cumulative distribution function [17,18] in statistical reliability distribution theory. From a probabilistic point of view, the use of Eq. (5) instead of an exponential function is equivalent to accounting for the distribution of lifetimes of reactive species in a manner different from that proper for reactions in homogeneous, three-dimensional systems.

In kinetics, the form of Eq. (3), once thought to be empirical, is now fully justified, in the most general way by the stochastic theory of reaction kinetics in dynamically disordered systems [19], and can be used in kinetic equations of any order. In the present article, we are interested in the use of $k(t)$ to describe the deceleratory α versus t curves, for the isothermal decomposition process of zinc leach residue [20,21].

The decomposition process of zinc leach residue from zinc winning process is very important for the economic and environmental reasons. In difference to the previous mostly described reduction processes, this thermal decomposition has been studied in a tubular furnace under a constant nitrogen gas flowing, at four different operating temperatures (600 °C, 750 °C, 950 °C and 1150 °C). Because of zinc leach residue is of the great interest for an environmental protection in metallurgical industry, the study of thermal decomposition is required. Decomposition of Zn-ferrite for O_2 generation by the concentrated solar radiation was performed in two steps [22]. The reduction plots of zinc ferrite solid solutions exhibited an initial linear rate followed by a gradual decrease in rate with increased percentage reduction. The solar decomposition of Zn-ferrite can be promoted with an increased temperature above 1477 °C.

The rates of reduction of dense pure zinc ferrite and zinc ferrite containing 1 wt% of CaO, MgO, MnO, and Al_2O_3 in solid solution reduced with H_2/N_2 gas mixtures have been investigated by Tong and Hayes [23] at temperatures between 500 and 1100 °C in order to establish an influence of impurities on reaction kinetics. The presence of impurity oxides in $ZnFe_2O_4$ solid solution influenced the conditions for formation of the porous iron morphology during the hydrogen reduction. Štrbac et al. [24] has presented a kinetic study of hydrometallurgical and hydrometallurgical processes employed for the recovery of zinc and removal of lead from a zinc plant residue ZPR. The maximum zinc recovery obtained during a hydrometallurgical treatment was 72% at 1300 °C.

It has been proven that a today's commercial plants for almost complete recovering zinc from zinc ferrite are based on fuming operations that reduces ferrite and vaporizes zinc. Such hydrometallurgical applications are using a reduction method with reaction media such as carbon monoxide, hydrogen and coke. The INDUTEC is such a high temperature process. In an induction furnace, zinc and other heavy metals are vaporized consuming high energy. The thermal reductive treatment in a Waelz process with partial destruction of the zinc ferrite produces a slag with very limited probability for use [25].

The above mentioned system, because of its industrial importance, the process of zinc leach residue decomposition in zinc production, has been under constant investigation in our laboratory, located in IME Process Metallurgy and Metal Recycling Institute (RWTH Aachen University).

The described kinetic approach, based on the dispersive kinetics laws and models [26–28], was the first time applied (in the current article) for this type of process, which is very important for the metallurgical industry, and which can also be implemented for any other process (which would be of interest for the metallurgy and hydrometallurgy), in order to elucidate the mechanism of the process, i.e., from the mechanistic point of view.

2. Experimental

2.1. Characterization methodology

The zinc leach residue was obtained from former company Ruhr-Zink, Datteln, Germany with a humidity of 23%. Before the experimental investigations, the samples were dried at the temperature of 120 °C over the night, in order to eliminate the humidity.

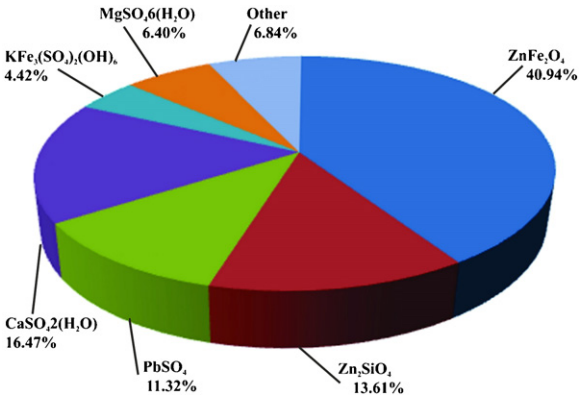

Fig. 1. Rietveld XRD analysis of the zinc leach residues ($ZnAl_2O_4$ is not presented in this figure, because its content is only 0.74% after the thermal decomposition, so it is assumed that the mentioned percentage is present in the frame of the "other" (6.84%) (see figure), together with other components, so that is not registered in this figure).

XRD (X-ray diffraction) phase analyses were done with a Bruker AXS Diffractometer Model D8. The mineralogical composition of neutral leach residue is shown in Fig. 1.

Rietveld XRD analysis of the tube furnace product after parameter optimization revealed the presence of zinc in the form of ZnO, $ZnAl_2O_4$ and $Ca_2ZnSi_2O_7$. This phase change made materials more soluble and suitable for the leaching process, which was previously reported [29]. The gaseous phases of PbO and SO_2 were formed during the thermal decomposition and they are removed with the nitrogen as carrier gas.

According to the phase analysis all zinc-ferrite is decomposed, iron is present only in the form of Fe_3O_4 and such decomposed sample has magnetic properties in difference to the original material. Magnesium was found as $Mg_2Si_2O_6$ and $Mg_3Al_2(SiO_4)_3$ phases (Fig. 2).

The chemical composition was determined by ICP (The inductively coupled plasma technique) on the dry sample averaged to the 18.6 Zn, 19.8 Fe, 6.7 Pb, 0.6 Cu, 0.2 Cd, 0.2 As, 10.9 Al, 7.3 S, 2.4 Ca, 2.1 Si (values in %) and 121 Ge, 558 Ag (values in ppm). In the case of the final reaction product, only the following four important elements were analyzed by ICP technique: 25.2 Zn, 22.5 Fe, 7.55 Al and 1.37 Pb (values in mass%).

An X-ray diffractometer (Siemens D 5000 Model) was used for characterization of the obtained particles. The investigated particles were agglomerated, different irregular forms and about 100 micrometer in the range. After thermal decomposition, the agglomeration was decreased, and the particles were round and polygonal. The degree of agglomeration and the shape of particles for treated

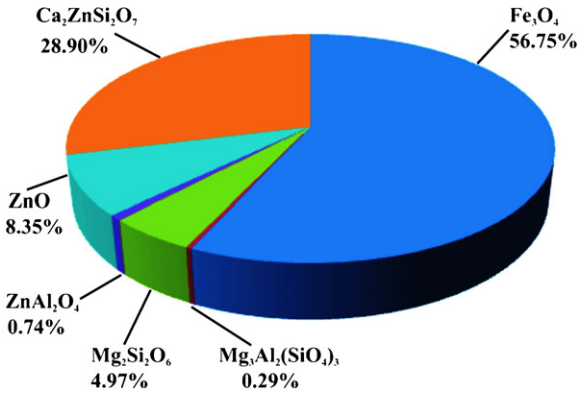

Fig. 2. XRD analysis of thermal decomposed leach residue (N_2 atmosphere–1150 °C).

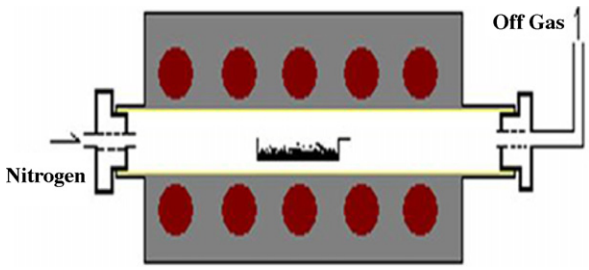

Fig. 3. The scheme of tubular furnace for thermal decomposition of zinc leach residue.

powder samples were determined using SEM (Scanning electron microscopy) analysis.

2.2. Isothermal measurements

After reaching the desired operating temperature, 1 gram of the zinc leach residue sample with agglomerated particles (the mostly rounded particles) was put into a tubular furnace, under a constant nitrogen gas, with a minimum flow rate, which was $\varphi = 1\,L\,min^{-1}$. Alumina crucible had been used in these experiments. The specimens were subjected to the thermal treatment at the constant temperatures between 600 and 1100 °C and durations between $t = 15$ and 60 min. After an injection of powder in the reaction tube at the aimed temperature, the reaction time was followed by the computation. After that, the considered specimen was taken out of the furnace and placed in the exicator. Each experiment at a given operating temperature was repeated twice. The weight results were noted as an average mass lost of the specimen. For the isothermal measurements, the total mass loss of the investigated sample was 77.36%. The scheme of tubular furnace for thermal decomposition of zinc leach residue is presented in Fig. 3. The intersection of the reaction tube within the tubular furnace, together with the presentation of the experimental sample is shown in Fig. 4.

3. Theoretical background

A key limitation of all KWW (Kohlrausch-Williams-Watts) and power-law based models lies in the physical ambiguity inherent in the unit-less time exponent, λ. For example, the time-dependent rate constant, k, used to describe the anomalous electron transit time dispersion in amorphous solids, an example of sub-diffusion,

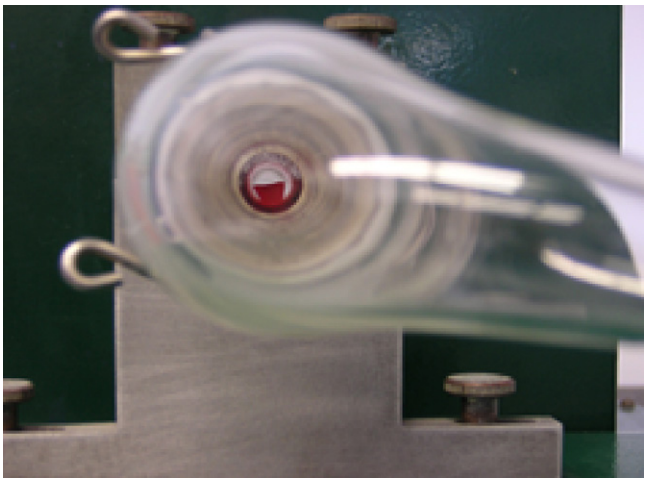

Fig. 4. Intersection of the reaction tube within the tubular furnace, together with presentation of the experimental samples.

can be obtained using the CTRW (the continuous time random walk) model. The functional form of this model can be presented by the following equation:

$$k = Bt^{\lambda-1} \quad 0 < \lambda \leq 1 \tag{6}$$

where B and λ represent the constants. Using Eq. (6), together with a first-order conversion model, yields the KWW relaxation function, Φ:

$$\Phi = \exp\left[-\left(\frac{t}{\tau_o}\right)^{\lambda}\right] \tag{7}$$

where

$$\tau_o = \left(\frac{\lambda}{B}\right)^{1/\lambda} \tag{8}$$

defines a relaxation time constant, whose λ value serves as a measure of the dispersive behavior of the conversion [3].

It can be pointed out, that if $\lambda = 1$, then $k = B$ (which represents a traditional, t-independent rate constant) and, consequently

$$\Phi = \exp(-Bt). \tag{9}$$

Eq. (9) reflects a classical (non-dispersive) Maxwell-Debye exponential decay profile. In contrast, Eq. (7) can be regarded as the result of a superposition of exponential decays (resulting from a multitude of parallel first-order conversions) that ultimately relates the stretched exponential decay observed in a wide variety of relaxation phenomena.

Using the variant of Eq. (7) we can obtained the Weibull distribution function for $\lambda > 1$, which is given in the form of the following equation:

$$\alpha = 1 - \exp\left[-\left(\frac{t}{\eta}\right)^{\theta}\right] \tag{10}$$

where θ is the shape parameter (which is the dispersive parameter ($\lambda \equiv \theta$)), and η is the scale parameter (which represents the relaxation time constant ($\tau_o \equiv \eta$)). In this aspect, Plonka [8] has demonstrated that the time dependence of the apparent activation energy, E_a, is given by equation:

$$E_a(t) = E_a^0 + (1-\theta)RT \ln\left(\frac{t}{\eta}\right). \tag{11}$$

In Eq. (11), E_a^0 is the t-independent (i.e., the classical/non-dispersive) initial value of the apparent activation energy, R is the gas constant, and T is the absolute temperature. Using Eqs. (10) and (11), the cumulative distribution function (cdf) ($f(E_a)$) and the density distribution function (ddf/pdf) ($g(E_a)$) has been derived elsewhere [8] and they can be represented as:

$$f(E_a) = 1 - \exp\left\{-\exp\left[\frac{\theta(E_a - E_a^0)}{(1-\theta)RT}\right]\right\} \tag{12}$$

and

$$g(E_a) = \left[\frac{\theta}{(1-\theta)RT}\right] \exp\left[\frac{\theta(E_a - E_a^0)}{(1-\theta)RT}\right] \exp\left\{-\exp\left[\frac{\theta(E_a - E_a^0)}{(1-\theta)RT}\right]\right\}. \tag{13}$$

The mean value of the apparent activation energy distribution (the first moment) can be defined in the form of the following expression [3]:

$$\left\langle E_a \right\rangle = E_a^0 - \gamma\frac{(1-\theta)RT}{\theta} \tag{14}$$

where γ is the Euler's constant ($\gamma = 0.577215665$). The reaction time implicitly exists in Eq. (14), via Eq. (15)

$$\left(\frac{t}{\eta}\right) = \exp\left[\frac{(E_a - E_a^0)}{(1-\theta)RT}\right] \tag{15}$$

for the condition when $E_a = \langle E_a \rangle$, so that t can be represented by an expression in the following form:

$$t = \eta \ \exp\left(-\frac{\gamma}{\theta}\right) = \eta \exp\left[\frac{\left\langle E_a \right\rangle - E_a^0}{(1-\theta)RT}\right]. \tag{16}$$

In accordance with Plonka [3], the dispersion of the considered distribution function (σ_{E_a}) is given by a following equation:

$$\sigma_{E_a} = \pi RT\frac{(1-\theta)}{\theta\sqrt{6}} \tag{17}$$

where $\pi = 3.14159265$. For $\theta = 1$, Eqs. (14) and (17) reduce to those proper for the classical kinetics, i.e.

$$\left\langle E_a \right\rangle = E_a^0 \tag{18}$$

and

$$\sigma_{E_a} = 0. \tag{18a}$$

3.1. The estimation of distribution parameters

3.1.1. The linear regression method

Linear regression ("ln-ln") method (LRM) [30] is a graphical method for calculating the values of the distribution parameters (θ and η) of the Weibull probability function with random variable t. This method is often used for the determination of θ and η, due to its simplicity and speed of calculation.

To get to the links between the two-parameter Weibull distribution function and the observed parameters (θ, η), Eq. (10) should be logarithmic twice, so the "ln-ln" transformations can be represented in the form:

$$\ln[-\ln(1-\alpha)] = \theta \ln\left(\frac{1}{\eta}\right) + \theta \ln t \tag{19}$$

The parameters of Weibull distribution function (θ, η) can be calculated from the linear dependence given by Eq. (19). The shape parameter (θ) and a scale parameter (η) can be calculated from the slope and intercept of the obtained straight line at a given operating temperature. The quality of linearization in the selected α range, can be checked on the basis of the obtained values of the squares of the linear correlation coefficient (R^2).

3.2. Dispersive kinetic model for describing deceleratory sigmoidal α–t curves

Based on Skrdla's [31] theoretical approach, in order to describe decelerator, sigmoid α–t curves, such as those relevant to denucleation (dissociation of critical nuclei) rate-limited process, including some crystal dissolutions and thermal decomposition processes, the following equation, which can be applied to solid-state kinetics, is evaluated:

$$\alpha = 1 - \exp[\alpha^* \cdot t][\exp(-\beta^* \cdot t^2) - 1] \tag{20}$$

Eq. (20) in origin is derived on the assumption of an M-B (Maxwell–Boltzmann)-like distribution of the apparent activation energies [31]. The M-B distribution of the apparent activation energies originates from molecular-level differences in the energies of either the reagent state or the activated state (A-S)/product species involved in defining the rate-determining step, depending on whether the conversion is deceleratory or acceleratory in

nature. The dispersion (i.e., the variation) in the apparent activation energy has been attributed to the differences in the molecular kinetic energies [3]. Note that the assumptions of a distribution of the apparent activation energies and a time-dependent rate constant are consistent with other dispersive kinetic treatments in the literature [3].

Eq. (20) contains only two "fit parameters", each with physically meaningful units, where α^* and β^*, have units of min^{-1} and min^{-2}, respectively. These constants may be referred to as "global rate parameters". Using Skrdla's assumption [31], that the only explicit—β values are valid in description of deceleratory α–t reaction profiles we can obtain the following set of dispersion relations:

$$E_a = E_a^0 + RT\beta^* t^2 \quad (21)$$

(t-dependent apparent activation energy)

$$k = \alpha^* \exp(-\beta^* t^2) \quad (22)$$

(t-dependent rate constant)and

$$\ln k = \ln \alpha^* - \beta^* t^2 = \left[\ln(A^{n^*-1}) + 2 - \frac{E_a^0}{RT}\right] - \beta^* t^2 \quad (23)$$

where A represents the Arrhenius-like pre-exponential (frequency) factor without entropic considerations, E_a^0 is the Arrhenius-like t-independent portion of the apparent activation energy barrier or (t-independent) potential component of the overall apparent activation energy [31]; n^* in Eq. (23) is a constant that relates to the dimensionality of the system and for the processes which exhibit the deceleratory α–t reaction profiles, the value of n^* in that cases is $n^* = 2$. That dimensionality is thought to reflect the fact that the distributed state in the rate-limiting step of de-nucleation-based processes (as the thermal decomposition), which pertains to the reactant species, is a two-dimensional nucleus. In Eqs. (21)–(23), if $\beta^* = 0$ and $n^* = 2$ (regarding to non-dispersive cases), then $k = \alpha^*$ and, consequently, the "textbook" kinetic relations are recovered [3].

Analogously to the Arrhenius equation, the value of E_a^0 can be calculated from the following equation [32]:

$$\ln\left(\frac{\alpha^*}{2}\right) = \ln\left(\frac{A}{2}\right) - \frac{E_a^0}{RT} \quad (24)$$

From Eq. (24), the slope of a plot of $\ln(\alpha^*/2)$ versus $1/T$ is given by $-E_a^0/R$ and the vertical axis intercept yields a value for $\ln(A/2)$, where it can be calculated A.

4. Results and discussion

The experimental isothermal decomposition data of the zinc leach residue at different operating temperatures (600, 750, 950 and 1150 °C) characterized by the conversion α–t curves (designated by symbols in Fig. 5) was modeled using the dispersive kinetic equation, which is given by Eq. (20).

The solid color lines in Fig. 5 were drawn using the dispersive kinetic parameters (α^* and β^*) of the best fits collected in Table 1. The quality of fit is given as the fit standard error, f_{se} in Table 1.

It can be seen from Table 1 that based on the obtained values of f_{se}, there is a very good agreement between the experimental conversion curves and decelerator α–t curves, calculated using Eq. (20). From the same table (Table 1), we can see that both parameters, α^* and β^*, increase with increasing of the operating temperature. Comparing the results in Fig. 5, we can see that as the operating temperature is increased, the decomposition generally occurs faster. Although, the value of β^* increases as the operating temperature is elevated, as one might expect for a rate constant (that it is the reciprocals of α^* values, which have units of min^{-1}, thus making them akin to the rate constant) that show a similar trend. It can be pointed out, that the particular increases of parameter β^* indicates a complex decomposition process of zinc leach residue, which may includes the two-step mechanism with a secondary nucleation process, taking place during the crystal growth, so that the site saturation condition is no longer fulfilled [31]. The driving force for the last mentioned process, increases with increasing values the dispersive parameter β^*, which is particularly manifested at the highest operating temperature (Table 1).

Table 2 shows the values of the dispersive parameter (θ), and the relaxation time constant (η) which were calculated using Eq. (19), for the dispersion kinetic model which is given by Eq. (10), at the different operating temperatures (600, 750, 950 and 1150 °C), in the case of the isothermal decomposition process of zinc leach residue.

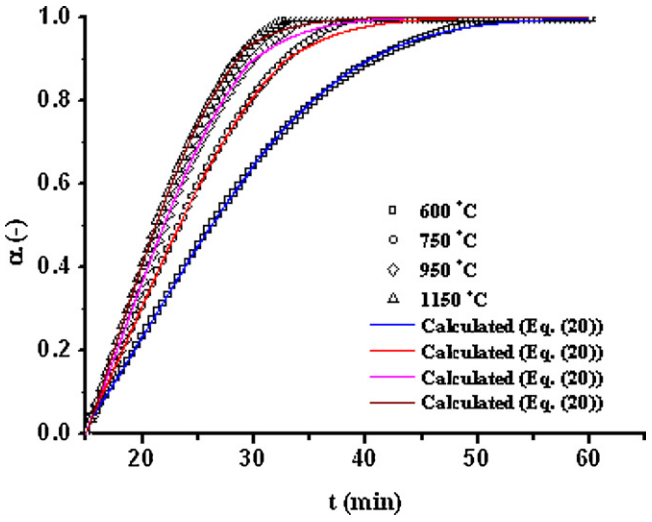

Fig. 5. The experimentally obtained conversion (α–t) curves (symbols) for the isothermal decomposition process of zinc leach residue, at the different operating temperatures (T = 600, 750, 950 and 1150 °C); the data fits (color solid lines) were performed using Eq. (20), for the dispersive kinetic parameters (α^* and β^*) presented in Table 1. (For interpretation of the references to color in this figure legend, the reader is referred to the web version of the article.)

Table 1
Dispersive kinetic parameters (α^* and β^*) for the isothermal decomposition process of zinc leach residue in an inert atmosphere at 600, 750, 950 and 1150 °C (Fig. 5), together with values of f_{se} at every considered operating temperature.

Temperature, T (°C)	α^* (min^{-1})	β^* (min^{-2})	f_{se}[a]
600	0.14685	3.00×10^{-4}	5.39×10^{-4}
750	0.22005	3.51×10^{-4}	8.68×10^{-4}
950	0.27029	3.69×10^{-4}	9.97×10^{-4}
1150	0.32558	3.75×10^{-4}	6.98×10^{-4}

[a] Fit standard error: $f_{se} = \sqrt{\sum_{i=0}^{N}(\alpha_{exp} - \alpha_{calc})^2/(N-p)}$, where N is the number of the experimental points, p is the number of parameters, α_{exp} is the experimental decomposition conversion and α_{calc} is calculated decomposition conversion.

Table 2
The values of dispersive parameter (θ), and the relaxation time constant (η) calculated using Eq. (19), for the dispersion kinetic model which is given by Eq. (10), at the different decomposition operating temperatures (600, 750, 950 and 1150 °C), in the considered conversion ranges ($\Delta\alpha$).

Temperature, T (°C)	$\Delta\alpha$	θ	η (min)	R^{2a}
600	0.16–0.95	2.96	30.28	0.99390
750	0.15–0.95	3.78	26.07	0.99271
950	0.15–0.95	4.32	24.17	0.99429
1150	0.16–0.95	4.74	23.41	0.99245

[a] The square of the linear correlation coefficient.

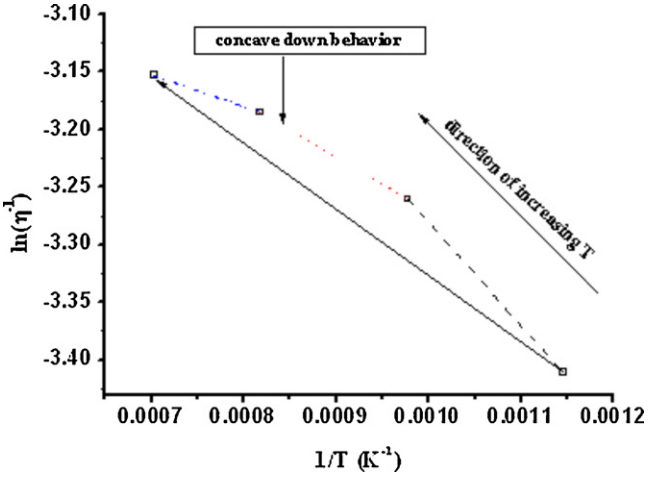

Fig. 6. The dependence $\ln(\eta^{-1})$ versus $1/T$ obtained for the isothermal decomposition process of zinc leach residue, at the different operating temperatures.

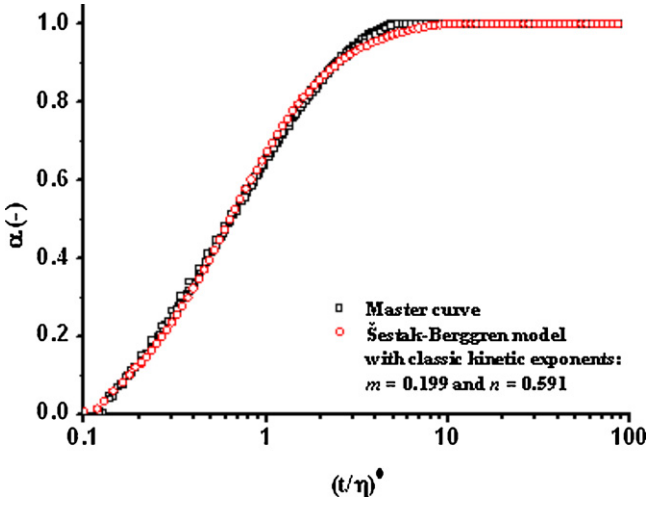

Fig. 7. The Master curve (α versus $(t/\eta)^{\theta}$ (symbol □)) of the experimental data for the decomposition process of zinc leach residue at the considered operating temperatures, presented in the coordinate system α versus $(t/\eta)^{\theta}$ on log scale; the corresponding α–$(t/\eta)^{\theta}$ curve fitted to the Šesták-Berggren kinetic equation (symbol ○), with the average values of the classic kinetic exponents, $m = 0.199$ and $n = 0.591$, are also presented on the same figure.

In the wide range of α values ($\Delta\alpha$), with the increasing of the operating temperature (T), the values of θ increase, and they are in the interval $2 < \theta < 5$. On the other hand, with the increase in the operating temperature, the values of η decrease (from $\eta = 30.28$ min at $T = 600\,^{\circ}$C to $\eta = 23.41$ min at $T = 1150\,^{\circ}$C) (Table 2). If the dependence of the logarithm of the reciprocal value of η ($\ln(\eta^{-1})$) in a function of $1/T$ shows deviation from the linearity (with concave down or concave up curves), this behavior may indicates the presence of thermally activated process, which exhibits non-Arrhenius dependence. Fig. 6 shows the dependence $\ln(\eta^{-1})$ versus $1/T$ obtained for the isothermal decomposition process of zinc leach residue, at the different operating temperatures.

It can be clearly seen from Fig. 6 that the dependence $\ln(\eta^{-1})$ versus $1/T$ evaluated for the considered decomposition process, expresses clearly the non-Arrhenius behavior, with a schedule of points that form a typical concave down curve, manifested by a positive deviation from the linear (Arrhenius) dependence. This situation indicates that the studied process has the characteristics of dispersion system, which is also confirmed by the values of the dispersive parameter (θ). Namely, the increase in θ value (Table 2), leads to an increase in the dispersion of conversion values of decomposition, in general. In addition, the appearance of conversion dispersion phenomena, will inevitably leads to a distribution of the apparent activation energies, for the investigated decomposition process of zinc leach residue. It should be noted that the changes in the value of the operating temperature, affects the degree of the dispersivity. Also, since the isothermal decomposition process of zinc leach residue gives quite high values of the dispersive parameter θ, where in this case we get the values of θ higher than four, then this result shows that the investigated process is very complicated. Likewise, this also suggests that the operating temperature (Table 2) significantly influences on the mechanism of the nucleation and the crystal growth for the producing of zinc in the form of zinc oxide [33].

Fig. 7 shows the "master curve" (α versus $(t/\eta)^{\theta}$ (symbol □)) of the experimental data for the decomposition process of zinc leach residue at considered operating temperatures (all curves are collapsed into one curve called the *master curve*), presented in the coordinate system α versus $(t/\eta)^{\theta}$ on log scale.

There are two reasons for showing the master curve in this coordinate system. First is for the exposures of the presence or absence of the induction period, especially at the very beginning of the considered process. Namely, from the each experimental α–t curve, can not be clearly seen whether or not there is an induction period. From the corresponding *master curve*, we can now detect the existence of a small induction period.

Also, Fig. 7 shows the corresponding α–$(t/\eta)^{\theta}$ curve fitted to the Šesták-Berggren kinetic equation (red symbol ○) [34,35], with the average values of the classic kinetic exponents, $m = 0.199$ and $n = 0.591$ [33] (where $f(\alpha) = \alpha^m(1-\alpha)^n$). The Šesták-Berggren kinetic equation subsists as a generalized operate based on the *logistic* function, $r{\cdot}\{\alpha(1-\alpha)\}$, which is customarily exploited to depict the case of population growth where r is the proportional factor of so called 'attractivity'. It consists of two essential but counteracting parts, the first one responsible for the "*mortality*" $\equiv\alpha^m$ (i.e., the reactant disappearance and the product formation) and the other for the "*fertility*" $\equiv(1-\alpha)^n$ (i.e., a kind of products' hindrance generally accepted as a counter-parting 'autocatalytic' effect [34]). The non-integral exponents, m and n, play thus the similar role as a broadly assumed non-integral dimensions common in the natural *world of fractals* [36]. The combination of two Šesták-Berggren kinetic exponents with values of $m = 0.199$ and $n = 0.591$ [33], corresponds to the Avrami kinetic parameter [15,16], with the value which is equal to the 1.41 [37].

Comparing the derived *master curve* and α–$(t/\eta)^{\theta}$ curve fitted with the Šesták-Berggren model [33], we can see that there is good agreement between these two curves. However, the advantage of the present approach is not in a better fit. It is in the sound physical basis of the dispersive kinetics and its phenomenological interpretation which is free from the mechanistic details [33] necessary in the classical approach.

To outline the phenomenological interpretation of Eq. (10) is the second reason of showing the master curve (Fig. 7). In order to find dependence $E_a = E_a(t)$ using Eq. (11), we must first calculate the value of E_a^0. Fig. 8 presents the dependence $\ln(\alpha^*/2)$ versus $1/T$, for the isothermal decomposition process of zinc leach residue in an inert atmosphere, for the operating temperatures in the range 600–1150 °C.

From Fig. 8, the global apparent activation energy was estimated at 14.6 ± 1.8 kJ mol^{-1} and the pre-exponential (frequency) factor obtained was $A = 1.1417$ min^{-1}. The obtained value of E_a^0 was higher than the value E_a (4.0 kJ mol^{-1}), which is calculated using the classical kinetic method, at exactly the right value of α ($\alpha = 0.50$) [33]. However, the evaluated value of E_a^0 is in a good agreement with

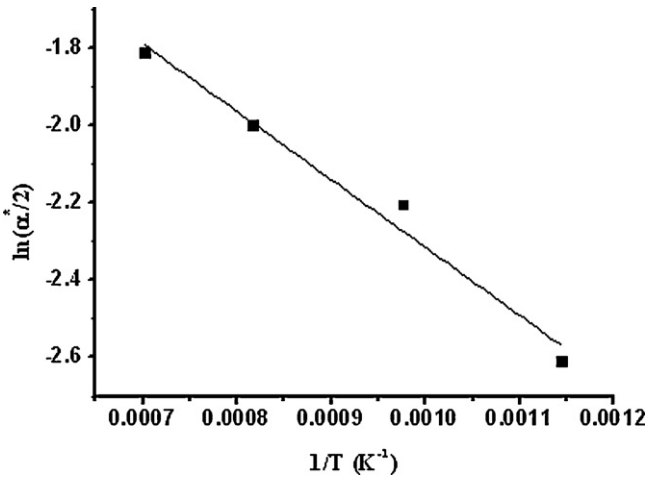

Fig. 8. The dependence $\ln(\alpha^*/2)$ versus $1/T$ for the isothermal decomposition process of zinc leach residue in an inert atmosphere, for the operating temperatures in the range of 600–1150 °C.

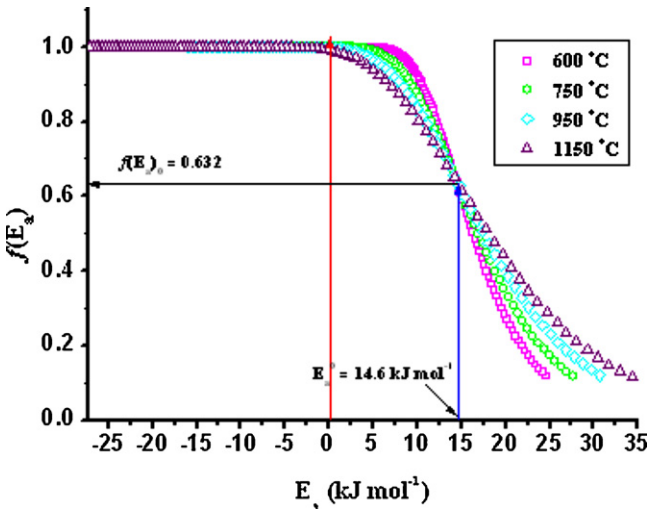

Fig. 10. The $f(E_a)$ versus E_a (Eq. (12)) for the decelerator α–t curves of the isothermal decomposition process of zinc leach residue, at the different operating temperatures (600, 750, 950 and 1150 °C).

the value of E_a calculated by the differential Friedman's [38] isoconversional method at the higher values of conversion ($\alpha \approx 0.85$) [33].

Fig. 9 shows the time dependence of the apparent activation energy (E_a), which is derived directly by using Eq. (11), at the different operating temperatures (T = 600, 750, 950 and 1150 °C), for the isothermal decomposition process of zinc leach residue.

It can be observed from Fig. 9, that the values of E_a decrease with an increasing of the reaction time (t), at all considered operating temperatures. It should be noted, the existence of transition from the positive scale values of E_a into the negative scale values of E_a at the very high operating temperature, so that we can *detect negative values* of $E_a(t)$.

From Fig. 9, we can notice the existence of reaction time interval, which is temperature dependent, with the negative values of E_a (examples of the negative values of the apparent activation energy can be found in scientific literature [39–45]). The observed isothermal process is complex as can be seen from the existing fact that the apparent activation energy changes during the process. This means that it consists of several parallel elementary reactions with strictly defined, but different apparent activation energies [33]. Their

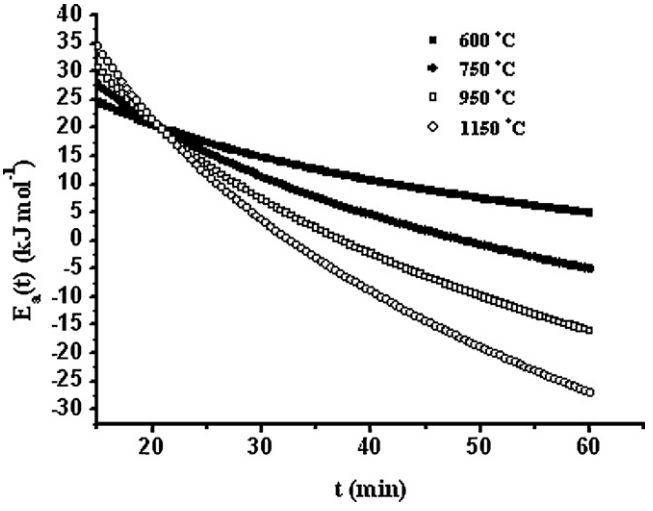

Fig. 9. The time dependence of the apparent activation energy (E_a) which is derives using Eq. (11) at the different operating temperatures (600, 750, 950 and 1150 °C), for the isothermal decomposition process of zinc leach residue.

contributions in the overall process are changed with reaction time and the operating temperature. In this case, the Arrhenius equation, even when applicable to each of the individual elementary reactions, it loses its original physical meaning when applied to the entire process. But despite that, the Arrhenius equation can be used for data processing, as well as any other mathematical function, but we must be careful when interpreting the obtained results. Formally, the existence of negative values of the apparent activation energy for the isothermal decomposition process of zinc leach residue, is a consequence of the occurrence of overlapping of already formed crystal seeds of the zinc oxide in the growth phase, and the secondary nucleation [46], which leads to a decrease in the rate of decomposition with increasing in the operating temperature. In this case, we have a typical *non*-Arrhenius behavior.

Fig. 10 represents the $f(E_a)$ versus E_a (Eq. (12)) for the decelerator α–t curves of the isothermal decomposition process of zinc leach residue, at the different operating temperatures (600, 750, 950 and 1150 °C).

It can be seen from Fig. 10 that the main findings of the $f(E_a)$–E_a curves, are located on the side of the positive values of E_a. All $f(E_a)$–E_a curves at every operating temperature, indicate the presence of asymmetric features. In addition, all the observed curves intersect at a characteristic point, which is the point of inflection with coordinates: $E_a = E_a^0 = 14.6\,\text{kJ mol}^{-1}$ and $f(E_a) = f(E_a)_0 = 0.632$ (Fig. 10). The observed characteristic point is fixed and corresponds to the value of E_a, which is exactly equal to the E_a^0 and the *cdf* ($f(E_a) = f(E_a)_0$) value equal to 0.632 [47], which is typical for the processes that were followed by nucleation and growth of new phases.

Fig. 11 shows the corresponding density distribution functions (*ddf*) ($g(E_a)$) (Eq. (13)) for the isothermal decomposition process of zinc leach residue, at the different operating temperatures (600, 750, 950 and 1150 °C).

The evaluated distributions are the asymmetric, centered at E_a^0 ($=E_{a,max}$) (Fig. 11), with pronounced low-energy tails that are not observed in a symmetrical Gaussian (normal) distribution. As θ increases, the *ddf* then expands, thereby covering a broader range of E_a values.

In all considered cases, however, the general shape of the distribution (Fig. 11) is opposite to that of the M-B (Maxwell–Boltzmann) distribution, which is skewed in the higher-energy direction.

The pre-exponential (frequency) factor (A) can be calculated by the straightforward method, through the relation, which connects

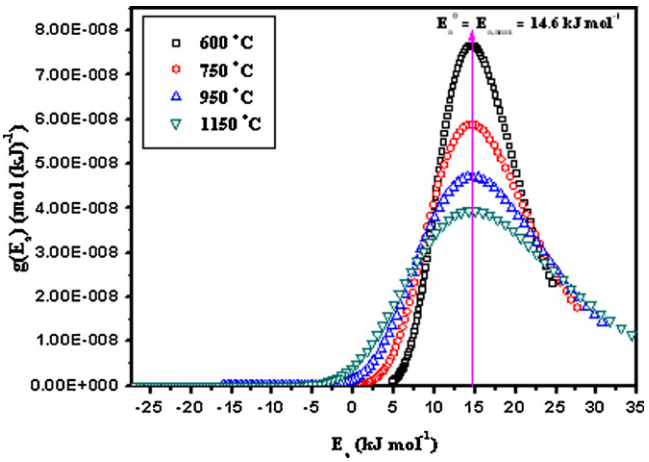

Fig. 11. The density distribution functions (*ddf*) ($g(E_a)$) (Eq. (13)) for the isothermal decomposition process of zinc leach residue, at the different operating temperatures (600, 750, 950 and 1150 °C).

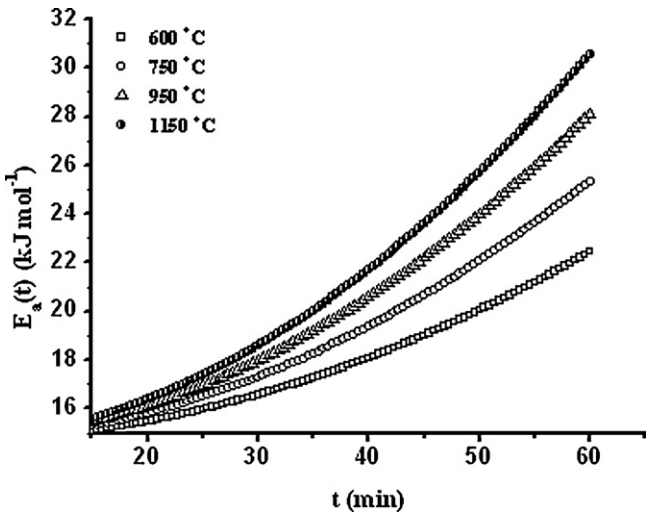

Fig. 12. The *t*-dependent apparent activation energy in a function of the reaction time (t), evaluated by using Eq. (21), for the isothermal decomposition process of zinc leach residue, at the different operating temperatures.

the maxima of the distribution ($g(E_a)$) curves ($E_{a,max}$) and the reaction time (t_{max}) which corresponds to the value of $E_{a,max}$, at the considered operating temperature T, in the form as

$$E_{a,\max} = RT \ \ln(At_{\max}) \tag{25}$$

and then from Eq. (25), after rearrangement, we finally get

$$\ln\ A = \frac{E_{a,\max}}{RT} - \ln\ t_{\max}. \tag{26}$$

For the isothermal decomposition process of zinc leach residue, using Eq. (26), the following values of A were obtained: $A = 1.2491\ \text{min}^{-1}$ ($T = 600$ °C); $A = 1.2147\ \text{min}^{-1}$ ($T = 750$ °C); $A = 1.1745\ \text{min}^{-1}$ ($T = 950$ °C); $A = 1.1482\ \text{min}^{-1}$ ($T = 1150$ °C). If we compare these values with the value of A, which is calculated using Eq. (24) ($1.1417\ \text{min}^{-1}$), we can see that there is a good agreement between the values of the pre-exponential factor. It may be noted that the best agreement is achieved at the highest operating temperature (1150 °C).

Table 3 shows the values of $\langle E_a \rangle$ and σ_{E_a} for $g(E_a)$ distributions calculated by Eqs. (14) and (17), for the isothermal process of zinc leach residue in an inert atmosphere, at the different operating temperatures (600, 750, 950 and 1150 °C).

From Table 3, we can see that with an increasing of the operating temperature, the values of both $\langle E_a \rangle$ and σ_{E_a} increase. Based on the obtained values of σ_{E_a}, we can clearly see that the distribution at the operating temperature of $T = 1150$ °C shows the overall width. On the other hand, based on the values of $\langle E_a \rangle$ (Table 3), we can see that $\langle E_a \rangle \neq E_a^0$, so that the condition $\sigma_{E_a} = 0$ is not fulfilled. Based on the obtained results, it can be concluded that the maximum dispersion of the system achieves at the highest operating temperature. The expansion of *ddf* and increased dispersion may be caused by the micro-environmental effects [48] that may arise during the complex process of zinc leach residue decomposition, especially at high values of operating temperature. It should be expected that the molecule of initial conformation surrounded by its own microenvironment possesses the characteristic activation barrier for conformational motion being partially a function of this microenvironment. The influence of these effects is followed by a substantial increase in the mean value of the apparent activation energy value (Table 3).

Table 3
The values of $\langle E_a \rangle$ and σ_{E_a} for $g(E_a)$ distributions calculated by Eqs. (14) and (17), for the isothermal process of zinc leach residue in an inert atmosphere, at the different operating temperatures (600, 750, 950 and 1150 °C).

Temperature, T (°C)	$\langle E_a \rangle$ (kJ mol^{-1})	σ_{E_a} (kJ mol^{-1})
600	17.4	−6.2
750	18.2	−8.0
950	19.1	−10.0
1150	20.0	−12.0

Fig. 12 shows the *t*-dependent apparent activation energy in a function of the reaction time (t), evaluated by using Eq. (21), for the isothermal decomposition process of zinc leach residue, at the different operating temperatures.

It can be observed from Fig. 12, that the E_a values increase with increasing of reaction time. Also, it is evident that there is an increase in E_a values with increasing of the operating temperature. If we compare the results in Fig. 12, with results that are shown in Fig. 9, we can see that there are obvious differences in the trend behavior of E_a values with changing t. In the first case (Fig. 12), the values of E_a increasing and they have positive values, while in the latter case (Fig. 9), the values of E_a decreasing, passing to the scale with negative values. The main essence of the existing differences lies in the nature of Eqs. (11) and (21). The *t*-dependence predicted by Eq. (21) is very different from the logarithmic one predicted by Eq. (11). Eq. (21) was obtained using the form of the *t*-dependent rate constant, which is presented by Eq. (22) [32].

Fig. 13 shows the *t*-dependent rate constants (Eq. (22)) as a function of t, for the isothermal decomposition process of zinc leach residue in an inert atmosphere, at the different operating temperatures (600, 750, 950 and 1150 °C).

It can be seen, that at all considered operating temperatures, the values of rate constants (k) decrease with increasing of reaction time. Looking at the change of the values of k with a change in the value of T, we can see that the value of k increases with increasing of the operating temperature. It can be pointed out, that Eq. (22) was derived based on the assumption of an underlying M-B (Maxwell–Boltzmann)-like distribution of the apparent activation energy [26]. The implications of that a priori assignment include the following concepts: (a) that past, present, and the future conversion times, as related via the *t*-dependent apparent activation energy, might all effectively coexist as if time were treatable like a spatial dimension and (b) the apparent activation energy barrier might be quantized, at least to some extent.

Based on the presented results, it should be clearly noted that if dispersion in the apparent activation energy/rate constant does not affect the zinc leach residue decomposition rate, the overall rate constant for the process $k(t)$ (Eq. (22)), becomes time-independent

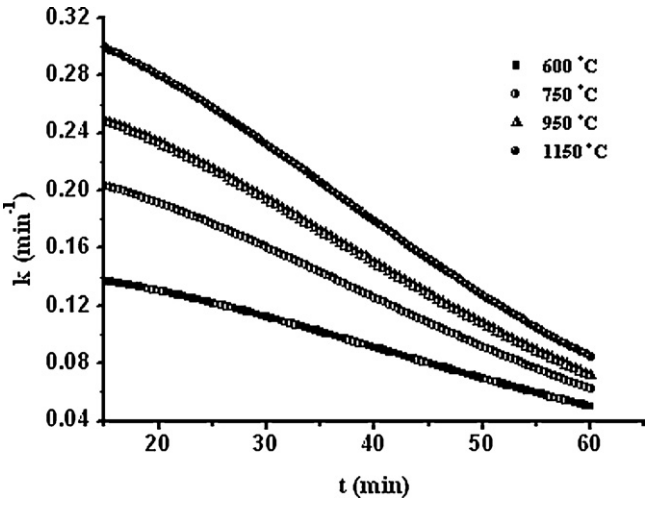

Fig. 13. The t-dependent rate constants (Eq. (22)) as a function of t, for the isothermal decomposition process of zinc leach residue in an inert atmosphere, at the different operating temperatures (600, 750, 950 and 1150 °C).

($\beta^* = 0$) and, hence the *single-valued*, as per the Arrhenius-Eyring definitions. For the cases, $k = \alpha^*$, a constant, essentially reducing Eq. (20) into the equation for the first-order kinetics ($\alpha = 1 - \exp(-kt)$).

On this basis, we can conclude that the above-mentioned fact does not apply in the case of the isothermal decomposition of zinc leach residue, because the present dispersion in the apparent activation energy values and also in the rate constant values obviously affect the decomposition rate (Figs. 12 and 13).

The dispersion in the apparent activation energy barrier is the direct result of "molecular motion" (which can vary from molecule to molecule), defines the distribution of the apparent activation energies for a given process. It is this distribution of apparent activation energies that, in turn, defines a time-dependent rate constant for the conversion. The time-dependent rate constant is important in describing the curvature observed in the experimentally obtained decelerator α–t curves (Fig. 5).

Fig. 14 shows the change in the values of time-dependent apparent activation energy ($E_a(t)$) as a function of decomposition conversion (α), for the isothermal decomposition process of zinc leach residue, at the different operating temperatures.

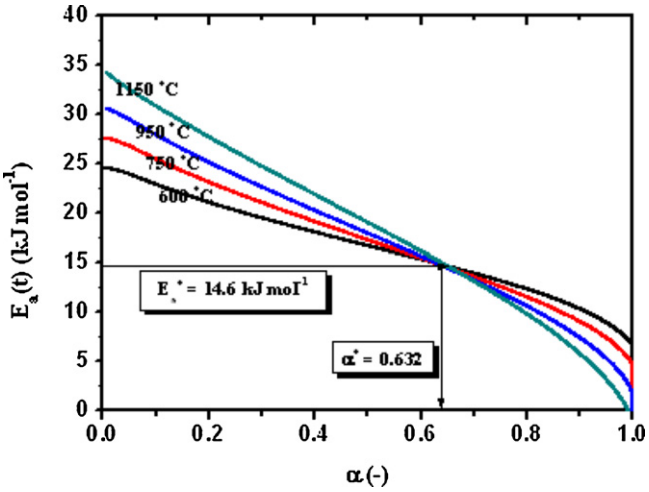

Fig. 14. The change in the values of time-dependent apparent activation energy ($E_a(t)$) (calculated by Eq. (21)) as a function of α, for the isothermal decomposition process of zinc leach residue, at the different operating temperatures (600, 750, 950 and 1150 °C).

It can be observed from Fig. 14 that at the all considered operating temperatures, the values of $E_a(t)$ decrease with an increasing of decomposition conversion (α). In this case, one should note an interesting phenomenon, that with an increasing of the operating temperature from 600 °C to 1150 °C, in the α range $\alpha = 0$–0.632 (0–63.2%) (Fig. 14), regarding to the point of intersection with the coordinates 0.632; 14.6 kJ mol^{-1}, the values of $E_a(t)$ (including the initial values of $E_a(t)$ at a given T: 24.6 (600 °C), 27.7 (750 °C), 30.7 (950 °C) and 34.3 kJ mol^{-1} (1150 °C)) increase, in the direction of increasing of the operating temperature. After the intersection point ($\alpha > 0.632$), the value of $E_a(t)$ decreases, in direction where the operating temperature increases ($\uparrow E_a(t)\,|14.6\,\text{kJ mol}^{-1}|\,\downarrow E_a(t)$—the opposite behavior) (Fig. 14). In fact, from the same figure (Fig. 14), we can see that the dependence of $E_a(t)$ on α, at all of the considered operating temperatures, actually changes its shape, from the concave into the convex functional dependence.

Based on these results, we can conclude that the decomposition process of zinc leach residue is a very complex process, which takes place through a system of parallel reactions, probably with variable dimensionality of the processes of nucleation and growth of a new phase (Fig. 14).

In this case, it may be set four kinetically important reactions (where each of these reactions is dominant in the different temperature regions [33]) for the isothermal decomposition process of the zinc leach residue, in the following forms, with subsequent discussion:

$$\text{(stage 1)}\quad PbSO_4 \rightarrow PbO + SO_2 + \tfrac{1}{2}O_2 \quad (T < 1000\,^\circ\text{C}) \tag{27}$$

The expected temperature range for this stage is 750 °C < T < 950 °C [49]. If we consider the dispersion parameter values (θ) listed in Table 2 (in the range of $3.78 \leq \theta \leq 4.32$), we can conclude that in this case, probably exists a three-dimensional growth of the formed PbO particles, with a constant nucleation rate. This result is the typical in case of obtaining of the large crystals, in the form of long and laminar structure [49].

$$\text{(stage 2)}\quad 3Fe_2O_3 \rightarrow 2Fe_3O_4 + \tfrac{1}{2}O_2 \quad (T < 1000\,^\circ\text{C}) \tag{28}$$

The reduction of Fe_2O_3 forming Fe_3O_4, with the expected temperature range of 400 °C < T < 650 °C. Bearing in mind the value of the parameter θ (=2.96 ≈ 3), we can conclude that in this case, we may expect the two-dimensional growth of the formed Fe_3O_4 particles, with the characteristic Fe_3O_4(111) interface [50].

$$\text{(stage 3)}\quad Zn_2SiO_4 \rightarrow 2ZnO + SiO_2 \quad (T < 1000\,^\circ\text{C}) \tag{29}$$

$$\text{(with additional step)}\quad ZnO \rightarrow Zn^\circ + \tfrac{1}{2}O_2 \quad (T < 1000\,^\circ\text{C}) \tag{29a}$$

The oxides reduction continues with increasing operating temperature, and zinc oxide will be produced at a operating temperature of about 800 °C [51] and at T above the 900 °C, mainly zinc vapor is formed as one of the main products. It can be noted, that the segregation of the silicate, i.e., the "liberation" of ZnO from the silicate previous to the actual reduction is not the rate limiting step [52]. In addition, the evolution of gaseous zinc and of oxygen is not limited by diffusion through a solid matrix.

$$\text{(stage 4)}\quad 3ZnO \cdot Fe_2O_3 \rightarrow 3ZnO + 2Fe_3O_4 + \tfrac{1}{2}O_2 \quad (T > 1000\,^\circ\text{C}) \tag{30}$$

The final production of zinc oxide (ZnO) is surely completed at the temperature of 1200 °C. ZnO·Fe_2O_3 (catalytic complex) is split at the very high temperatures (T > 1000 °C) in a non-complex form as $ZnO + Fe_3O_4 + \frac{1}{2}O_2$. ZnO·$Fe_2O_3$ likely to be autocatalytic decomposed into ZnO and other chemical species, which significantly reduces the energy barrier for a given process. However, in the case of autocatalytic reaction, the reaction rate is strongly

influenced by the concentration of the formed product. In the considered decomposition process, the overall decomposition reaction rate is strongly depends on the amount of the obtained zinc oxide (ZnO). It should be noted the following fact, that the molecular oxygen has to evolves to complete the decomposition process, which is effectively implemented in the presence of oxide, such as Fe_2O_3 [53]. In addition, based on very high value of the dispersive parameter at 1150 °C (θ = 4.74, which is close to value of 5 (Table 2)), we can expect the effect of branching, especially in response to the initial reagent that has autocatalytic properties (Eq. (30)). In this case we get the maximum dispersion in the values of the apparent activation energy (Fig. 11). The formation of the branches is the nucleation of new crystals on the columnar facets of ZnO crystals. One might expect the existence of the line defects under the branched crystals. These line defects that are created, serve as the pin-points for the secondary nucleation to occur. Branch growth on the single crystalline ZnO further supports the idea that the new crystals are mostly formed on the defect sites, such as edges or holes.

It can be pointed out, that in this case, the reduction of the surface energy will be the highest when the best match between the substrate and the crystallizing substance is achieved. This situation may be created, when both the substrate and the crystallizing substance are the same/or the almost same, referred to as the secondary nucleation.

In our previously reported results, the kinetic model which can best describes the investigated decomposition process, from the classical kinetic approach, is the two-parameter autocatalytic Šesták-Berrgren model [34]. Málek [36] pointed out that the classical nucleation-growth equation (Avrami or Johnson-Mehl-Avrami (JMA) equation) is actually a special case of this two-parameter Šesták-Berrgren (SB) model, and thus SB equation ($d\alpha/dt = k(T)\cdot\alpha^m(1-\alpha)^n$) represents a plausible alternative description for the crystallization process. The increasing value of parameter m indicates a more important role of the precipitated phase on the overall kinetics. However, the temptation to relate the values of m and n to a reaction mechanism can be doubtful and should be avoided [36]. The value and wide applicability of the SB equation surpasses in the light of the single-step approximation. The conversion function, $f(\alpha) = \alpha^m(1-\alpha)^n$, is able to describes both, acceleratory and decelerator α–t curves, as well as the nth order reaction α–t curves.

In general, the values of kinetic exponents may not reflect the reaction mechanism. On the other hand, they enable to describe kinetic data and modeling the kinetics of the overall process without a deeper insight into its mechanism.

Due to the empirical nature of the SB equation, the relatively large number of fit parameters and given the complexity of many solid-state processes, it may be difficult to correlate small differences in the values of these constants (m and n) with any well-defined change in the mechanism. This is especially true if the mechanism is known to change over the course of the reaction or the transformation (a mechanistic change is typically observed as a change in the activation energy with conversion), as in our case, for the isothermal decomposition of zinc leach residue in an inert atmosphere.

Because of this fact, the SB equation provides purely formal description of the kinetic description of the isothermal decomposition process of zinc leach residue, as presented in our previous work [33].

However, in this article, it was shown that Eq. (20) better fitted the experimentally obtained α–t curves of the isothermal decomposition of zinc leach residue (Fig. 5), than the SB kinetic equation with kinetic parameters m = 0.199 and n = 0.591 [33]. The dispersive kinetic approach for the investigation of the complex isothermal decomposition process of zinc leach residue provides more detailed information about the reaction mechanism, rather than the conventional approach, in order to describe the process using the SB equation.

Namely, the statistical approach which yielded the two-parameter model equation (Eq. (20)) can be used as a better alternative in modeling the investigated process and for the detailed mechanistic description of the same. The model presented in this article may offer a more physically meaningful approach for the treatment of the kinetic data compared to that of standard (i.e., non-dispersive) kinetic model.

Some of the advantages of the dispersive kinetic model in the kinetic analysis of the complex decomposition process of zinc leach residue in an inert atmosphere, over existing kinetic models, may include the high quality of the data fits (Table 1) and the use of only two fit parameters, each with physical units.

5. Conclusions

The formalism of dispersive kinetics is applied for the decomposition process of zinc leach residue in an inert atmosphere. The isothermal decomposition has been studied in a tubular furnace under a constant nitrogen gas flowing, at the four different operating temperatures (T = 600 °C, 750 °C, 950 °C and 1150 °C). It was found that the dispersive kinetic model in the form of equation $\alpha = 1 - \exp[\alpha^* t][\exp(-\beta^* t^2) - 1]$ (α^* and β^* are "fit parameters", with physically meaningful units) more successfully modeled the complex decomposition process, than classic (non-dispersive) Šesták-Berggren (SB) kinetic model. It was shown that the system heterogeneity is responsible for giving rise to the underlying distribution of the apparent activation energies (E_a) ultimately imparts a time dependence to the specific rate of the decomposition conversion.

Also, it was found, that the increase in the values of the parameter β^* with an increasing of the operating temperature, indicated the occurrence of the secondary nucleation process, taking place during the crystal growth. In addition, it was shown that the overall decomposition process exhibit the non-Arrhenius behavior, which is manifested by a positive deviation from the linear (Arrhenius) dependence. Also, in this study, it was shown that the dispersion in the apparent activation energy/rate constant affects the zinc leach residue decomposition rate, and in this case, the overall rate constant for the investigated process, becomes time-dependent. Because of this fact, the single-valued condition for E_a is no longer fulfilled. From the obtained results, we can conclude that the investigated system exhibits the non-single-exponential kinetics. This behavior is characteristic for the systems where the rates of the overall process are faster than some slower, internal conversion or the environmental effects.

Acknowledgments

The authors would also like to thank the Ministry of Science and Environmental Protection of Serbia, under the Project 172015 (Bojan Janković).

We like to thank Deutsche Forschungsgemeinschaft DFG in Bonn for financial support of the project FR 1713/13-1: Zn-recovery from steel making dusts – Kinetics and mechanism of thermal zinc-ferrite phase decomposition (Srećko Stopić, Aybars Güven, and Bernd Friedrich).

References

[1] S. Glasstone, Textbook of Physical Chemistry, D. van Nostrand Co., Princeton, 1959, pp. 25–45.
[2] A. Plonka, Time-Dependent Reactivity of Species in Condensed Media. Lecture Notes in Chemistry, No. 40, Springer-Verlag, Berlin Heidelberg, New York, London, Paris, Tokyo, 1986, pp. 1–151.

[3] A. Plonka, Dispersive Kinetics, Kluwer Academic Publishers, Dordrecht, The Netherlands, 2001, pp. 1–220.
[4] A. Khawam, D.R. Flanagan, Solid-state kinetic models: basics and mathematical fundamentals, J. Phys. Chem. B (110) (2006) 17315–17328.
[5] S. Vyazovkin, C.A. Wight, Model-free and model-fitting approaches to kinetic analysis of isothermal and nonisothermal data, Thermochim. Acta (340–341) (1999) 53–68.
[6] J. Šesták, Diagnostic limits of phenomenological kinetic models introducing the accommodation function, J. Therm. Anal. Calorim. 36 (1990) 1997–2007.
[7] N. Koga, J. Málek, J. Šesták, H. Tanaka, Data treatment in non-isothermal kinetics and diagnostic limits of phenomenological models, Netsu Sokutei 20 (1993) 210–223.
[8] A. Plonka, Dispersive kinetics in condensed phases, Ann. Rep. Prog. Chem. Sect. C. Phys. Chem. 85 (1988) 47–75.
[9] V. Chernyak, M. Schulz, S. Mukamel, Stochastic-trajectories and non-Poisson kinetics in single-molecule spectroscopy, J. Chem. Phys. 111 (1999) 7416–7425.
[10] E. Barkai, Y.J. Jung, R. Silbey, Theory of single-molecule spectroscopy: beyond the ensemble average, Annu. Rev. Phys. Chem. 55 (2004) 457–507.
[11] L.K. Schirra, B.S. Tackett, M.L. Blumenfeld, O.L.A. Monti, Single molecule power-law behavior on a crystalline surface, J. Chem. Phys. 131 (2009) 124702–124708.
[12] M. Kuno, D.P. Fromm, H.F. Hamann, A. Gallagher, D.J. Nesbitt, Nonexponential, blinking kinetics of single CdSe quantum dots: a universal power law behavior, J. Chem. Phys. 112 (2000) 3117–3120.
[13] A. Plonka, Recent developments in dispersive kinetics, Sci. Rev. 25 (2000) 109–218.
[14] N. Koga, H. Tanaka, Accommodation of the actual solid-state process in the kinetic model function I. Significance of the non-integral kinetic exponents, J. Therm. Anal. Calorim. 41 (1994) 455–469.
[15] M. Avrami, Kinetics of phase change I. General theory, J. Chem. Phys. 7 (1939) 1103–1112.
[16] M. Avrami, Kinetics of phase change II. Transformation-time relations for random distribution of nuclei, J. Chem. Phys. 8 (1940) 212–224.
[17] W. Weibull, A statistical representation of fatigue failures in solids, Trans. R. Instit. Technol., Stockholm, Sweden (27) (1949) 1–9.
[18] W. Weibull, A statistical distribution function of wide applicability, J. Appl. Mech. 18 (1951) 293–296.
[19] A. Plonka, A. Paszkiewicz, Kinetics in dynamically disordered systems: time scale dependence of reaction patterns in condensed media, J. Chem. Phys. 96 (1992) 1128–1133.
[20] K.L. Bhat, K.A. Natarajan, T. Ramachandran, Electroleaching of zinc leach residues, Hydrometallurgy 18 (1987) 287–303.
[21] R. Alizadeh, F. Rashchi, E. Vahidi, Recovery of zinc from leach residues with minimum iron dissolution using oxidative leaching, Waste Manag. Res. 29 (2011) 165–171.
[22] H. Kaneko, T. Kodama, N. Gokon, Y. Tamura, K. Lovegrove, A. Luzzi, Decomposition of Zn-ferrite for O_2 generation by concentrated solar radiation, Solar Energy 76 (2004) 317–322.
[23] L. Tong, P. Hayes, Mechanisms of the reduction of zinc ferrites in H_2/N_2 gas mixtures, Mineral Process. Extrac. Metall. Rev. 28 (2006) 127–157.
[24] N. Štrbac, I. Mihajlović, V. Andrić, Ž. Živkovic, A. Rosić, Kinetic investigations of two processes for zinc recovery from zinc plant residue, Canadian Metall. Quart. 50 (2011) 28–34.
[25] G. Kaupp, F.E. Martinez, H. Ren, V.D. Jaramillo, H. Zoz, High kinetic processing of EAF dust and a new hydrometallurgical recycling scheme, Metall 62 (2008) 819–823.
[26] P.J. Skrdla, R.T. Robertson, Semiempirical equations for modeling solid-state kinetics based on a Maxwell–Boltzmann distribution of activation energies: applications to a polymorphic transformation under crystallization slurry conditions and to the thermal decomposition of $AgMnO_4$ crystals, J. Phys. Chem. B 109 (2005) 10611–10619.
[27] P.J. Skrdla, R.T. Robertson, Dispersive kinetic models for isothermal solid-state conversions and their application to the thermal decomposition of oxacillin, Thermochim. Acta 453 (2007) 14–20.
[28] P.J. Skrdla, R.T. Robertson, Use of dispersive kinetic models to describe the rate of metal nanoparticle self-assembly, Chem. Mater. 20 (2008) 3–4.
[29] S. Stopić, B. Friedrich, Kinetics and mechanism of thermal zinc-ferrite phase decomposition, in: Proceeding of EMC 2009, 28 June–1 July, Innsbruck, Austria, 2009, pp. 1167–1181.
[30] P. Bhattacharya, R. Bhattacharjee, A study on Weibull distribution for estimating the parameters, J. Appl. Quant. Methods 5 (2010) 234–241.
[31] P.J. Skrdla, Crystallizations, solid-state phase transformations and dissolution behavior explained by dispersive kinetic models based on a Maxwell–Boltzmann distribution of activation energies: theory, applications, and practical limitations, J. Phys. Chem. A 113 (2009) 9329–9336.
[32] P.J. Skrdla, A collision theory-based derivation of semiempirical equations for modeling dispersive kinetics and their application to a mixed-phase crystal decomposition, J. Phys. Chem. A 110 (2006) 11494–11500.
[33] B. Janković, S. Stopić, A. Güven, B. Friedrich, Kinetic analysis of isothermal decomposition process of zinc leach residue in an inert atmosphere. The estimation of the apparent activation energy distribution, Mineral Process. Extrac. Metall. Rev. (2012), Revised article GMPR-2012-0067R1 18 May 2012, under review.
[34] J. Šesták, G. Berggren, Study of the kinetics of the mechanism of solid-state reactions at increasing temperatures, Thermochim. Acta 3 (1971) 1–12.
[35] P. Šimon, Fourty years of the Šesták–Berggren equation, Thermochim. Acta 520 (2011) 156–157.
[36] J. Málek, Kinetic analysis of crystallization processes in amorphous materials, Thermochim. Acta 355 (2000) 239–253.
[37] J. Šesták, J. Málek, Diagnostic limits of phenomenological models of heterogeneous reactions and thermal analysis kinetics, Solid State Ionics 63–65 (1993) 245–254.
[38] H.L. Friedman, Kinetics of thermal degradation of char-forming plastics from thermogravimetry-application to a phenolic resin, J. Polym. Sci. C 6 (1964) 183–195.
[39] W. Primak, Kinetics of processes distributed in activation energy, Phys. Rev. 100 (1955) 1677–1689.
[40] E.V. Waage, B.S. Rabinovitch, Simple and accurate approximation for the centrifugal factor in RRKM theory, J. Chem. Phys. 52 (1970) 5581–5584.
[41] J.D. Hoffman, G.T. Davis, J.I. Lauritzen Jr., The rate of crystallization of linear polymers with chain folding, in: N.B. Hannay (Ed.), Treatise on Solid State Chemistry, vol. 3, Plenum, New York, 1976, pp. 497–614, Chapter 7.
[42] M. Gibbs, J. Evetts, J. Leake, Activation energy spectra and relaxation in amorphous materials, J. Mater. Sci. 18 (1983) 278–288.
[43] M. Mozurkewich, S. Benson, Negative activation energies and curved Arrhenius plots. Theory of reactions over potential wells, J. Phys. Chem. 88 (1984) 6429–6435.
[44] S. Vyazovkin, N. Sbirrazzuoli, Estimating the activation energy for the non-isothermal crystallization of polymer melts, J. Therm. Anal. Calorim. 77 (2003) 681–686.
[45] S. Vyazovkin, J. Stone, N. Sbirrazzuoli, Hoffman-Lauritzen parameters for non-isothermal crystallization of poly (ethylene teraphthalate) and poly (ethylene oxide) melts, J. Therm. Anal. Calorim. 80 (2005) 177–180.
[46] P.H. Lindenmeyer, Surface area and secondary nucleation theory, Nature 269 (1977) 396–397.
[47] J. Málek, The kinetic analysis of non-isothermal data, Thermochim. Acta 200 (1992) 257–269.
[48] A. Marcinek, J. Gębicki, A. Płonka, Microenvironmental effects in solid-state reactions. Dispersive kinetics of conformation-dependent charge delocalization in aliphatic diamine radical cations, J. Phys. Org. Chem. 3 (1990) 757–759.
[49] S.A.A. Sajadi, A comparative investigation of lead sulfate and lead oxide sulfate study of morphology and thermal decomposition, Am. J. Anal. Chem. 2 (2011) 206–211.
[50] A.M. Bataille, L. Ponson, S. Gota, L. Barbier, D. Bonamy, M. Gautier-Soyer, C. Gatel, E. Snoeck, Characterization of antiphase boundary network in $Fe_3O_4(111)$ epitaxial thin films: Effect on anomalous magnetic behavior, Phys. Rev. B 74 (2006) 155438–155449.
[51] E. Saage, U. Hasche, Optimisation of the Waelz process at the B.U.S. Zinkrecycling Freiberg GmbH, World Metall.–*ERZMETALL* 57 (2004) 138–142.
[52] A. Weidenkaff, A. Reller, A. Steinfeld, Solar production of zinc from the zinc silicate Ore Willemite, J. Solar Energy Eng. 123 (2001) 98–101.
[53] S. Ju, Y. Zhang, Y. Zhang, P. Xue, Y. Wang, Clean hydrometallurgical route to recover zinc, silver, lead, copper, cadmium and iron from hazardous Jarosite residues produced during zinc hydrometallurgy, J. Haz. Mater. 192 (2011) 554–558.